NASA- CR 168055

DEVELOPMENT PROGRAM ON A SPINDT COLD-CATHODE ELECTRON GUN

Final Report

November 1982

By: C.A. Spindt, Senior Research Engineer
Engineering Sciences Laboratory

Prepared for:

National Aeronautics and Space Administration
Lewis Research Center
21000 Brookpark Road
Cleveland, Ohio 44135

NASA Contract NAS3-22469

SRI Project 2590

SRI International
333 Ravenswood Avenue
Menlo Park, California 94025
(415) 859-6200
TWX: 910-373-2046
Telex: 334 486

SRI International®

SRI International

CR 168055

DEVELOPMENT PROGRAM ON A SPINDT COLD-CATHODE ELECTRON GUN

Final Report

November 1982

By: C.A. Spindt, Senior Research Engineer
Engineering Sciences Laboratory

Prepared for:

National Aeronautics and Space Administration
Lewis Research Center
21000 Brookpark Road
Cleveland, Ohio 44135

NASA Contract NAS3-22469

SRI Project 2590

Approved:

Fred J. Kamphoefner, Director
Engineering Sciences Laboratory

Earle D. Jones, Vice President
Advanced Development Division

SRI International®

CONTENTS

ILLUSTRATIONS

TABLES

I INTRODUCTION

This report summarizes the past year's work in an ongoing program at SRI International (SRI) to develop a thin-film field-emission cathode (TFFEC) array and a cold-cathode electron gun based on the emitter array. The objective is the production of a microwave-tube gun that uses the thin-film field-emission cathode as an electron source.

During this report period, the project effort was directed to fabricating, testing, and delivering state-of-the-art cathodes to the National Aeronautics and Space Administration (NASA), Lewis Research Center (LeRC), for evaluation; and to improving reliability and increasing the tip-packing density of the arrays, thereby increasing the cathode's current-density capability.

The TFFEC is based on the well-known field-emission effect and was conceived to exploit the advantages of that phenomenon while minimizing the difficulties associated with conventional field-emission structures, e.g. limited life and high voltage requirements. Field emission has been shown to follow the Fowler-Nordheim equation (Fowler and Nordheim, 1928):*

$$J = \frac{AF^2}{t^2(y)\phi} \exp - \frac{Bv(y)\phi^{3/2}}{F}$$

where J is the emission-current density in A/cm^2, A and B are constants, F is the field at the tip, ϕ is the work function in eV, and v(y) and t(y) are slowly varying functions of y where

$$y = \frac{3.79 \times 10^{-4} F^{1/2}}{\phi} \quad .$$

Both v(y) and t(y) are tabulated in the literature (Burgess at al., 1953). The field at the tip is

$$F = \beta V \text{ volts/cm} \quad ,$$

where V is the voltage applied to the diode structure and

$$\beta = f(r,R,\theta)cm^{-1} \quad .$$

---

*References are listed at the end of this report.

The relationship between β and the tip radius (r), the anode-to-tip spacing (R), and emitter-cone half angle (θ) is complex (Dyke and Dolan, 1956) and difficult to determine accurately; for the purpose of our work we note that as r, R, and θ become smaller, β increases. Thus, smaller cathode-anode structure reduces the voltage required for a given emission current.

The conventional field emitter, shown in Figure 1, consists of a short segment of fine wire (usually tungsten) etched electrolytically at one end of a sharp point (i.e. small r). The segment is mounted on a hairpin filament for support and is then cleaned by passing current through the hairpin filament and heating the tip to incandescence. After cooling, the point supplies cold electron emission when a positive voltage is applied to a ring or aperture anode spaced at a macroscopic distance (R) (approximately 1.0 mm) from the emitter tip. At the point surface, the electric field required for field emission is on the order of 10^7 V/cm; so, with the local field enhancement resulting from the sharpness of the tip, anode potentials of the order of kilovolts are usually required for field emission from a conventional emitter structure. Positive ions formed at the anode or between the anode and the sharp emitter are directed toward the tip by the curved field lines. Some of these ions have energies in the keV range and can therefore roughen or sharpen the tip by sputtering. The sputtering rate is determined by the rate of ion formation (which is directly related to the local vacuum pressure and emission current drawn) and by the ion energies (which depend on the applied voltages). Tip sharpening by ion sputtering during operation increases the local field (for the same applied voltages) and thus progressively increases the emission current and the sputtering rate until an arc or resistive heating of the tip leads to its destruction. This effect places a limit on useful lifetimes for conventional emitters; however, Brodie (1975) has shown that the sputtering effect can be greatly reduced if one can lower the emission voltage below

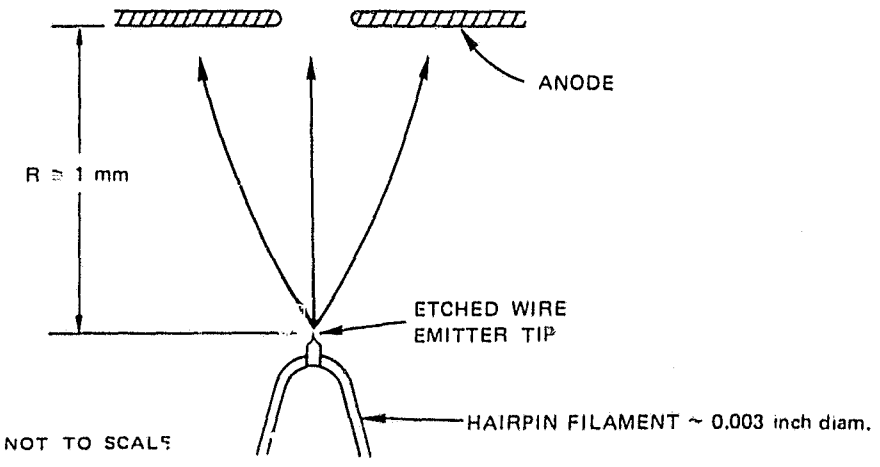

FIGURE 1 CONVENTIONAL FIELD EMITTER AND ANODE

150 V; reduction of the applied voltage to 50 V may effectively eliminate the sputtering.

Another difficulty with the etched-wire emitter is that fabricating large arrays of tips for high-current applications would be very difficult, and in dense arrays neighboring tips would shield each other electrostatically. Thus, large emitter-arrays that produce high current densities have not yet been achieved by these means.

In an effort to overcome these difficulties, the field emission cathode shown in Figure 2 was developed at SRI. This cathode consists of a conductor/insulator/conductor sandwich with dielectric thickness of approximately 1.5 μm, holes approximately 1.5 μm in diameter in the top conductor (metal gate film), undercut cavities in the dielectric layer, and metal cones within the cavities.

Field emission is obtained from the tips of the cones when the tips are driven to a negative voltage with respect to the gate film. Because of the field enhancement of the tip (small r) and the close spacing between the rim of the hole in the gate film and the tip (small R), potentials of only 100 V to 200 V are required across the sandwich for large field-emission currents. In addition, dense arrays of the tips can be operated without the tips influencing one another, because the gate film surrounds each cone and prevents reduction of the electric field by mutual shielding between the tips.

This configuration also reduces the problem of ion bombardment from other high voltage electrodes, because the tips are well shielded electrostatically by the gate film; that is, the equipotentials contoured about the tip are essentially confined within the cavity, and the equipotentials between the gate film and other external acceleration electrodes are essentially uniformly spaced and plane parallel. Thus, unlike the etched-wire configuration, most ions formed between the gate film and an external acceleration electrode are directed toward the gate film rather than the tip. The volume of ionization between the gate film and the tip is very small; any ions formed within this region will have low energies (100 to 200 eV) and will be unlikely to cause significant sputtering damage by striking the tip. This assumption appears to be well justified; experimental results show currents averaging over 50 μA per tip for over 65,000 hours from a 100-tip array. The tips are operating at room temperature and unknown pressure, but probably in the 10^{-9}-torr range.

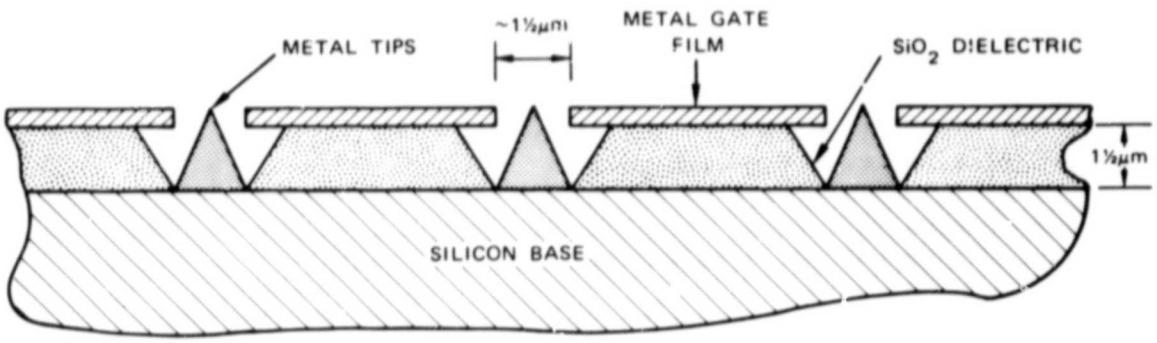

(a) SCHEMATIC OF A THIN-FILM FIELD-EMISSION CATHODE (TFFEC) ARRAY

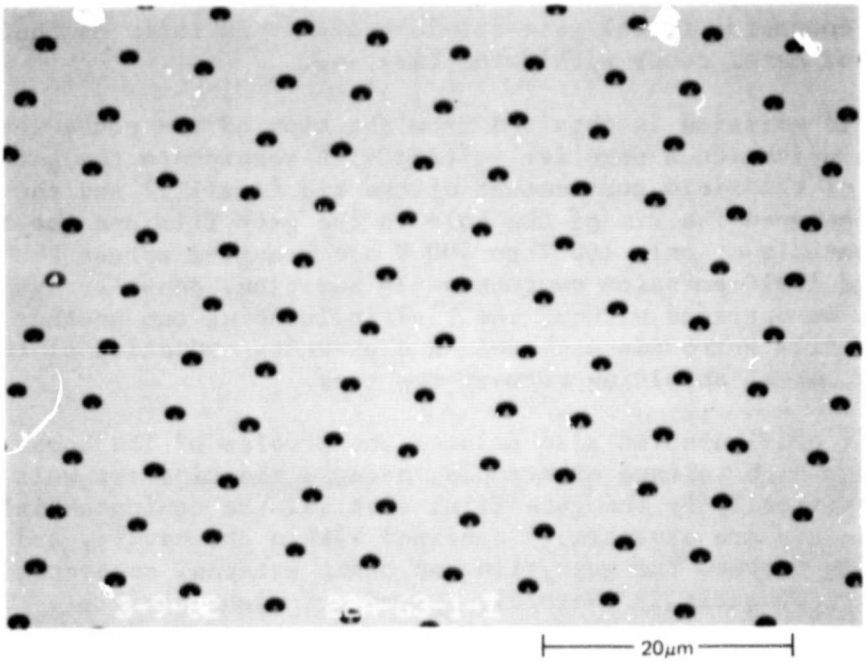

(b) SEM MICROGRAPH OF TFFEC ARRAY

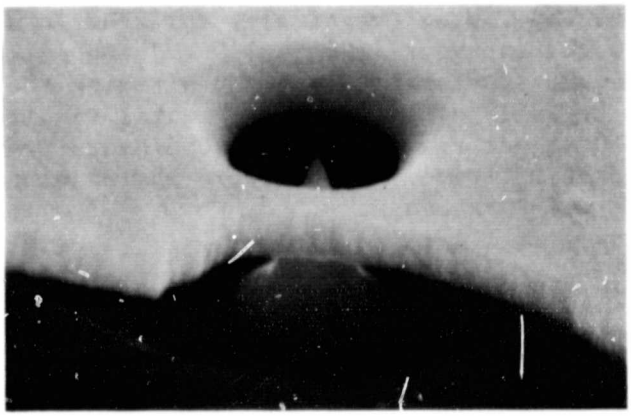

(c) SEM MICROGRAPH OF TFFEC CATHODE

FIGURE 2 THIN-FILM FIELD-EMISSION CATHODE

II PURPOSE OF THE EXPERIMENTAL PROGRAM

The objective of the program is the development of a field-emission array cathode suitable for use in a microwave-tube gun structure. The tasks that were the objectives of this phase of the program were:

- Fabricating, testing, and delivery of state-of-the-art cathodes for in-house experiments at NASA Lewis Research Center and the Naval Research Laboratories (NRL).
- Advancing the fabrication technology in order to produce a cathode that has increased tip packing density, and thus is capable of producing increased emission-current density.
- Investigating failure mechanism encountered when the cathode is used in various configurations.
- Investigating methods for fabricating wedge-shaped field emission cathodes and arrays of such cathodes.

III STATE-OF-THE-ART CATHODES

The state-of-the-art cathode has been defined as a 5000-tip array covering an area 1-mm in diameter on a 2.5-mm square silicon chip. The tip packing density is 6.4×10^5 tips/cm^2. Tip spacing is 12.7-μm between centers. All the cathodes tested on this phase of the program are described in the Appendix. Cathodes delivered to NASA and NRL are listed in Table 1. Of the 32 cathodes delivered, 11 were delivered untested at NASA's request. Deliveries were made only when requested so that the cathodes shipped could always be the most up-to-date available.

Cathodes are stored in two ways prior to shipping: mounted in TO-5 headers held in aluminum racks and stored in ordinary plastic parts-boxes or stored in aluminum trays that are kept in pyrex petri dishes (cathodes that are awaiting test, or that have been tested in our moly/alumina demountable test headers). The petri dishes and plastic boxes are stored on a laminar flow bench.*

Before shipping, a protective stainless-steel cover is placed over the TO-5 header, the cathodes are wrapped in aluminum foil, and the foil-wrapped cathode is placed in a glass bottle. The bottle is purged with dry nitrogen before the lid is secured. No cathodes have been physically damaged by shipping; however, the conditions of storage and shipping may introduce surface contamination that can cause changes in the operating characteristics of the cathodes.

*These rather crude storage conditions will be the subject of a future study to determine whether the cathodes should be stored under a more controlled environment.

Table 1

CATHODES DELIVERED

Cathode Number	Mount	Gate Current (μA)	Applied Voltage	Emission (mA)	Tips Blown	Shorts	Cathodes Tested
20A-55-1-F	LeRC	-100	130	30	0	0	x
20A-70-1-G	TO-5	+20	92	20	2	0	x
-I	TO-5	+65	60	15	25	0	x
-K	LeRC	--	--	--	--	--	--
-R	None	--	--	--	--	--	--
-S	None	--	--	--	--	--	--
-X	LeRC	--	--	--	--	--	--
20A-70-2-V	TO-5	<1	160	20	0	0	x
-W	TO-5	<1	160	20	0	0	x
-X	TO-5	<1	152	20	1	0	x
20A-71-3-C	TO-5	+60	150	20	7	0	x
-D	TO-5	+15	170	50	11	0	x
-H	LeRC	-18	200	20	2	0	x
-K	LeRC	-14	205	20	29	0	x
-O	TO-5	--	--	--	--	--	--
-R	TO-5	--	--	--	--	--	--
-X	TO-5	-2	195	20	25	0	x
20A-81-1-D	TO-5	<1	180	20	6	0	x
-F	TO-5	+10	145	20	20	0	x
-G	TO-5	-10	150	20	8	0	x
-I	TO-5	-5	164	20	55	0	x
-Q	None	-16	175	20	30	0	x
-R	None	-4	170	20	21	0	x
20A-82-1-R	TO-5	--	--	--	--	--	--
-S	TO-5	--	--	--	--	--	--
-T	TO-5	--	--	--	--	--	--
20A-82-2-H	TO-5	--	--	--	--	--	--
-J	TO-5	--	--	--	--	--	--
-R	TO-5	--	--	--	--	--	--
20A-82-3-C	TO-5	<1	200	10	9	0	x
-D	TO-5	<1	200	10	8	0	x
20A-112-5-D	None	<1	128	54	9	0	x

IV FABRICATION TECHNOLOGY

A. State-of-the-Art Cathodes

The state-of-the-art cathode array during this phase of the program [a 5000-tip array with tips on 12.5-μm centers (6.4×10^5 tips/cm^2)] covers an area 1 mm in diameter on a p-type, 0.01 Ω-cm <111> silicon chip that is nominally 2.5-mm square. This cathode type has been designated "type 20A" in the cathode series. (See Figure 3 and Tables 2 and 3.) Several other configurations that have been made or planned are also described in Tables 2 and 3.

The basic cathode-fabrication process has been changed and modified several times during preceding phases of the program. Developments continue as the research progresses and new technologies become available. The basic state-of-the art cathode-fabrication process at the end of this phase is as follows:

- Two-inch-diameter silicon wafers are oxidized to a depth of about 1.5 μm in a wet oxygen atmosphere at about 1000°C.
- Molybdenum is deposited over the oxide to a depth of about 4000 Å using an electron-bombardment-heated evaporator.
- The 2-inch (5-cm) wafer is cut into 1/2-inch (1.27-cm) square substrates with a dicing saw.
- An electron-sensitive resist, poly(methyl-methacrylate) or PMMA, is spun onto the substrates, and the desired pattern of holes is exposed in the PMMA using the SRI-developed screen-lens parallel-beam electron-lithography system. Typically, 25 patterns on 0.25-cm centers are formed on the 1.25-cm square substrate.

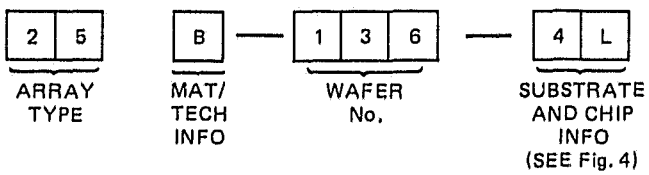

FIGURE 3 CATHODE IDENTIFICATION CODE EXAMPLE:

25 B - 136 - 4 L is a 16-tip array on 12.7-μm centers, fabricated on p-type <111> silicon, using reactine ion beam etching (RIBE). The wafer is number 136, the substrate is number 4, and the chip is "L" (Figure 4).

Table 2

ARRAY TYPES

Code	Tips	Centers (μm)
20	5,000	12.7
21	1*	
22	20,000	6.35
23	100	12.7
24	400	6.35
25	16	12.7
26	40	6.35
27	40,000	4.5
28	10,000	9
29	32	9
30	5,000*†	
31	16*†	
32	64*†	
33	100*†	
34	100	9

*Wedges, 0.1 mm long
†Wedges, 10 μm long with ~10 μm spacing between them. Packing density 6.4×10^5 wedges/cm^2

Table 3

ARRAY MATERIAL AND TECHNOLOGY

Array Code	Description
No letter	p-type (100), wet chemistry
A	p-type (111), wet chemistry
B	p-type (111), RIBE etch
C	n-type (111), wet chemistry
D	n-type (111), RIBE etch

- The PMMA is developed and the molybdenum film is etched away where it is exposed by the holes developed in the PMMA layer.
- The silicon dioxide layer is etched through to the silicon substrate where it has been exposed by the holes etched in the molybdenum film.
- The PMMA is removed, and cones are formed in the holes using a dual deposition technique developed at SRI for this purpose (Spindt, 1981).
- The gate film pattern is then etched using photolithography. Typically, this pattern consists of 25 pads 1.78-mm square, with the cathode array centered in the pad.
- The 1.27-cm square substrate is then cut into the desired number of cathode chips to correspond with the pattern that was formed with the screen lens. The state-of-the-art cathode is cut into 25 cathode chips, each about 0.25-cm square, with the 1.78-mm square molybdenum pad and cathode array centered on the chip.
- The chips are cleaned and mounted for testing. These processes were described in detail in previous reports on this development program (NASA CR-159866, CR-159570, CR-134888, and CR-165401).

B. Advanced Fabrication Processes

During this phase of the development program, there were four major improvements in the fabrication process outlined above:

- Gate film deposition
- Gate film patterning
- Active area patterning
- Wedge-shaped emitters

1. Gate Film Deposition

The first improvement was to modify the gate-film-deposition apparatus so that the gate film could be deposited on a complete 2-inch diameter wafer, without cutting the wafer into 1/2-inch square substrates prior to the deposition. The significance of this modification is in the interface between the deposited molybdenum gate film and the grown silicon dioxide layer. If the surface of the oxide is contaminated before the molybdenum deposition, the gate film's adherence will be poor; as a result, the oxide etch used to form the holes will undercut the molybdenum excessively and weaken the cathode structure. Contamination can also cause pinholes in the deposited film, which frequently lead to electrical breakdown, and contamination that is trapped between the molybdenum gate and the oxide layer could produce local gas bursts

on the cathode during operation, which can cause erratic performance and electrical breakdown.

With the apparatus modified to accomodate 2-inch-diameter wafers, the wafer can go straight from the oxidation furnace to the gate-film-deposition station without a cooling period. The wafer is baked in the vacuum system to 900°C before the gate film is deposited, so that any gases that are absorbed during transport from the oxidation furnace to the evaporation system will desorb before the molybdenum gate film is deposited.

The molybdenum is deposited with the wafer at 400°C. The wafer is then cut into 1/2-inch squares with a dicing saw. The surface is coated with thick PMMA before dicing so that sawdust will not adhere to the molybdenum film, but will be washed away with the PMMA when it is removed. This adds no new surface contamination because the next step in the fabrication sequence is to coat the 1/2-inch squares with another layer of PMMA for the screen-lens exposure of the hole patterns.

2. Gate Film Patterning

The second major change in the fabrication process was in the technique used for patterning the gate film on the 1/2-inch square substrate. In the original work, the gate film was deposited through a mask that defined 25 gate-film pads in a 5x5 array, as shown in Figure 4. It was then necessary to deposit aluminum over the open oxide between the pads to connect the gate films so that they were not electrically isolated. (The holes are etched in the molybdenum using electron beam lithography, so there must be electrical contact between all the pads.)

During the most recent phase of the development program, the process was changed so that the molybdenum gate film is deposited over all the substrate surface uniformly; the aluminum deposition to connect the pads is not needed. The hole patterning and cone formation are done with the entire 1/2-inch substrate covered with molybdenum and then--as a last step prior to dicing the substrate into 25 separate cathode chips--the gate film is patterned using photolithography. The holes are so small (~1.5-μm diameter) that the photoresist spans the holes and protects the cones from the molybdenum etch that defines the gate pads.

This technique has been very helpful, because we can now process all 25 cathodes on a single substrate as one piece, and then dice the substrate into 25 separate cathodes as a final step, which greatly improves uniformity and fabrication efficiency.

Three technological problems had to be overcome to implement this technique. The first was that the gate films did not adhere well to the substrate, although the failure did not become obvious until the

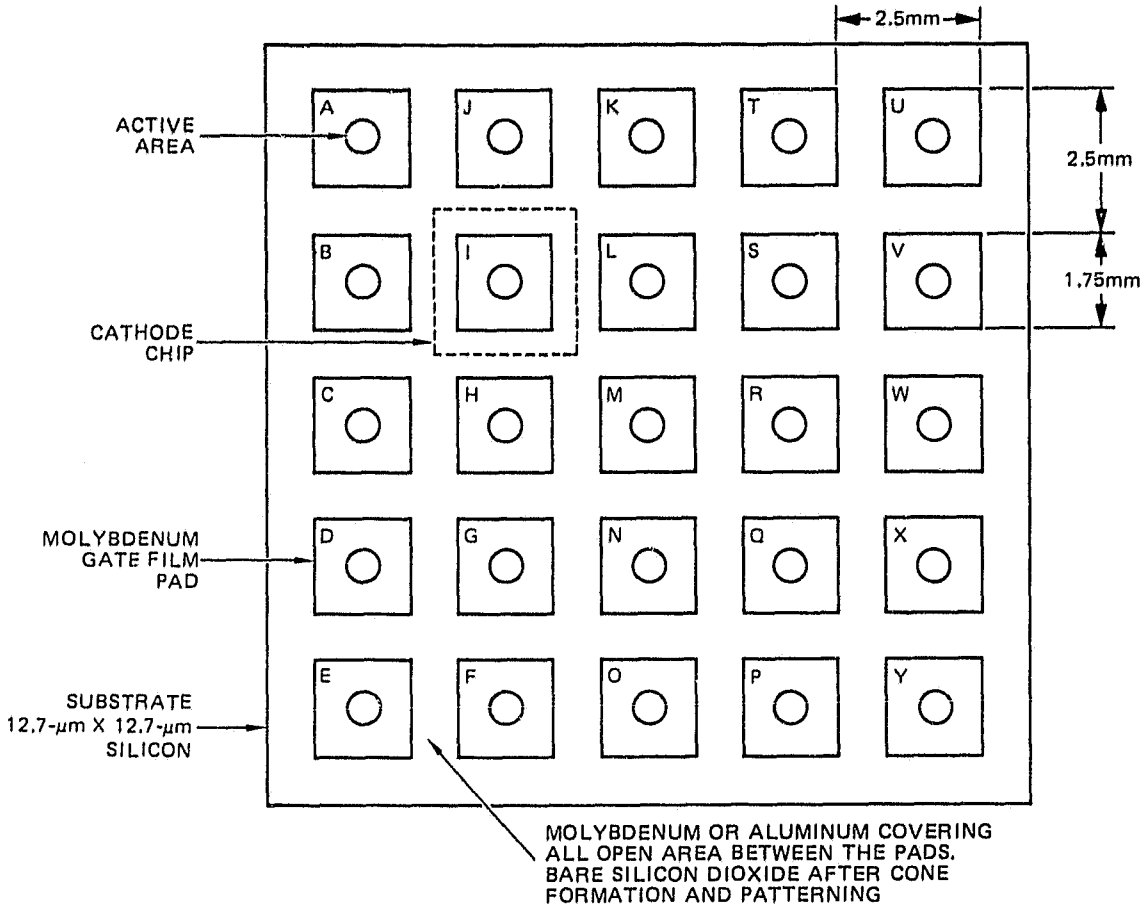

FIGURE 4 LAYOUT OF 25 CATHODE CHIPS ON A 1.27-cm (1/2-INCH) SQUARE SILICON SUBSTRATE

substrate had been through all the processing except dicing. At this point, because of the stress on the gate film caused by the build-up of the cone formation film on the gate film's surface, the gate film broke up and pulled away from the oxide. We were then able to observe that the oxide had been catastrophically attacked by the oxide etchant where it was supposed to have been protected by the gate film, as though the gate film had been porous. A careful study of the process revealed that jigging made to handle the new substate holders used for depositing the gate film over the entire substrate surface had been built so that the jig inadvertently touched the oxide surface to be coated with the molybdenum gate film; this was contaminating the surface. New jigs were made and the problem disappeared.

The second difficulty was in the photolithography process. It was necesssary to use a negative resist in order to see the hole array when aligning the photomask with the substrate. Negative resists are generally difficult to remove cleanly and require harsh chemicals that

tended to attack the molybdenum gate film and the cones. We also found that the resist had to be very thick in order to span the holes so that the cones would not be etched away. Furthermore, when the photomask was placed on the surface for exposure of the pattern, the cones damaged the resist, and thus many cones were subsequently etched away.

The difficulties were overcome by using a positive resist that dissolved readily in acetone, using a high-viscosity resist for increased thickness, making jigging that spaced the photomask a few micrometers above the substrate surface, and using iron oxide masks that are transparent to some visible light but not ultraviolet (UV). Thus we can align the mask visually by looking through the part that is opaque to UV.

The third difficulty was in the dicing process. Dicing is done after the 25 cathodes on a substrate have been completely fabricated. It is important that no sawdust gets onto the cathode surface and into the holes, because it is impossible to remove except by etching. Etching silicon at this stage of the fabrication etches the silicon under the cones and causes the cones to fall out. This problem was solved by coating the substrate with very thick PMMA and then dicing the substrate with the dicing saw. The heavy PMMA holds up to the sawing, and all the sawdust is on top of the PMMA. It is then possible to dissolve the sawdust with a silicon etch, because the cathode is protected by the PMMA. The final step is to remove the PMMA and clean the cathode chips.

This PMMA coating technique is also used to protect the 2-inch wafers during dicing into 1/2-inch substrates, as mentioned earlier.

3. Active Area Patterning

The third process improvement was the development of a double resist technique to define the active area of the cathode. Prior art required that we modify our screen-lens electron-beam lithography system to change the size of the active area. This was cumbersome and interfered with the flow of state-of-the-art cathodes because it disrupted the electron lithography process.

We therefore developed a dual resist technique. The idea is to do a normal state-of-the-art hole array exposure on the electron-sensitive PMMA resist (5000 tips on 12.7-μm centers over a 1-mm-diameter area), develop the resist, and then spin a photoresist (e.g. KTI 1350J or 809) over the developed PMMA. A photomask can then be aligned over the hole pattern to expose a pattern in the photoresist and to open a window over the holes that are to be etched in the molybdenum gate film. For example, a 50-μm square photomask can be lined up over the 5000-tip array to open a window over a 4x4 array of holes on 12.7-μm centers. This is done visually in a standard mask aligner. The photoresist is exposed and developed, leaving the desired area of the PMMA with its hole pattern open for processing. The PMMA is then descummed in an asher (oxygen plasma) and the molybdenum etched through the holes

in the PMMA resist. The rest of the 5000 holes (which are covered by the photoresist) do not etch.

Using this technique, we can form any shaped pattern of holes within the 1-mm diameter array without changing anything in our screen-lens electron-beam lithography system. Small area cathodes fabricated with this process should be ready for test early in the next phase of the program.

4. Wedge-Shaped Emitters

The last major improvement in our processing technology was to upgrade the screen-lens electron-beam exposure system in order to lithograph arrays of lines (as well as dots) in the PMMA electron-sensitive resist.

The lines are used to develop a wedge-shaped, rather than the cone-shaped, emitter. Using the wedge-shaped emitter may do more than increasing the cone packing density to achieve improved current density from a given active area.

If one assumes that each emitter tip in an array has a tip radius (r) of 1000 Å and an emission cone (θ) of up to 30° from the axis of the cone, the emitting area (A) per cone is $A = 2\pi r^2(1-\cos\theta)$, or about 10^{-10}cm^2. The total emitting area for the state-of-the-art 5000-tip array is thus 5×10^{-7} cm^2.

Now consider a 5000-slot array with slots 1.5-μm wide, and 10-μm long wedges in the slots. These could be fabricated in the same area that is occupied by the state-of-the-art 5000-tip cathode, and the wedges can be formed by the same process by which the cones are formed. If each wedge has a radius of curvature (r) of 1000 Å and a length (L) of 10 μm, and we assume a 30° emitting half angle (θ), the total emitting area (A) per wedge is $A = \theta\pi rL \times 1.1 \times 10^{-2}$ or about 10^{-8} cm^2, for a total emitting area over the 5000 slots of 5×10^{-5} cm^2. This is an improvement of two orders of magnitude over the area available with the cone array. From this simple analysis, it is clear that the wedge geometry should be investigated.

It has been shown (Spindt, 1980) that the wedge can be formed by the same process as the cones. The difficulty is in forming an array of slots. There are three ways to form an array of slots (lines) with electron beam lithography: raster scanning or vector scanning with a conventional electron-beam lithography system (both serial operations), fabricating a screen with the desired slot-packing density and length, or scanning the existing screen-lens-system array of beamlets across the substrate. The serial scanning systems would require far too much time and are too sophisticated for such a simple pattern. Fabricating a screen for our screen lens system is feasible; however, this approach is not very flexible and would require changing the screen lens for every new pattern. The most flexible approach is to scan

the array of beamlets across the sustrate using SRI's existing screen-lens electron-beam lithography system.

The screen lens system had already been modified for mechanical scanning: Manipulators were added to translate the screen and substrate in order to do step and repeat exposures to increase the packing density of the hole array. Packing densities of up to 2.5×10^6 tips/cm^2 (20,000 tips in an area 1 mm in diameter) have been demonstrated using this step and repeat technique (Spindt, 1980), with manual positioning of the stage supporting the screen and substrate. The hole patterns can be positioned to accuracies of about 0.01 μm with this apparatus (manually), because of the very large demagnification of the system.

The system (shown in Figure 5) consists of a tungsten hairpin filament cathode, a grid cap, drift space, screen lens, and target. Each hole in the screen functions as an aperture and tiny lens when voltages are applied as shown. The electron optical theory developed for this configuration predicts that the object (virtual cathode just in front of hairpin) will be (de)magnified in the ratio $M = Z_i/2Z_o$, where M = (image size)/(object size), Z_i is the distance from the screen to the image (target), and Z_o is the distance from the screen to the object (cathode). Thus, with the configuration used [i.e. Z_o = 24 inches (61 cm) and Z_i = 1/16 inch (1.5 mm)], we have $M = 1.3 \times 10^{-3}$. Then, because the system had a 2000 line/inch screen [i.e. 0.0005-inch (12.7-μm) center-to-center spacing], and we wished to print an array of holes on 0.00025-inch (6.35-μm) centers, we had to do four exposures while moving the image 0.00025 inches (6.35 μm) on the substrate between exposures. Furthermore, we had to move 0.00025 inches (6.35-μm) in directions that are parallel to the orthogonal orientation of the lines on the 2000 line/inch screen.

It is clearly very difficult to move the target 0.00025 inches (6.35 μm) between each of four exposures and still get precise positioning of the pattern, especially when the manipulation must be done on the target in a vacuum chamber. However, we could take advantage of the (de)magnification factor (M) and move the object (cathode) a distance (d_o) in a direction parallel to one of the sets of screen wires and cause the image to move some proportional distance (d_i) that will be $d_i = Md_o$. Because we knew that we wanted d_i to be 0.00025 inch (6.35 μm) and M was calculated to be 1.3×10^{-3} from the system geometry, we could estimate the distance the cathode had to be moved for the first trial as $2.5 \times 10^{-4}/1.3 \times 10^{-3} = 0.1923$ inches (4.88 mm).

Because of the configuration of the screen lens system, it is much easier to move the screen/target combinaton together than to move the cathode. The screen/target combination was mounted on a microscope stage whose dial indicators were graduated in 0.001-inch (25-μm) increments; the positioning of the image on the target thus could be done to within 1.4×10^{-6} inch (0.03 μm) when the (de)magnification factor is taken into account.

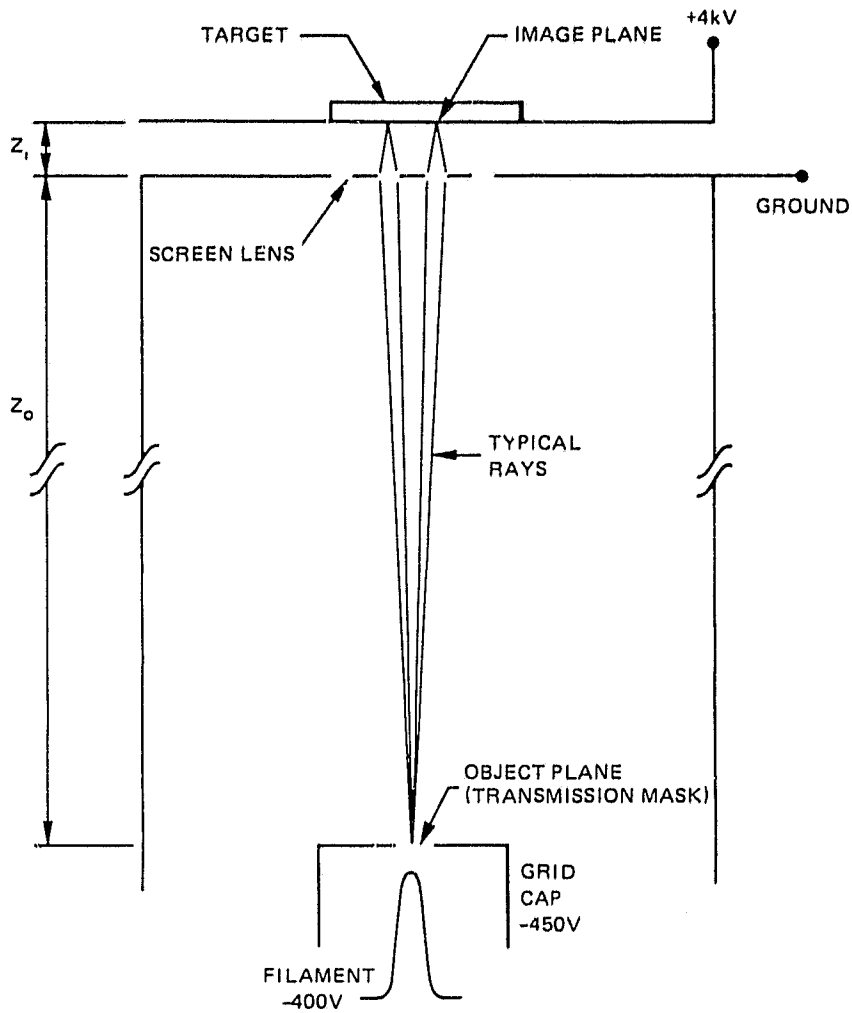

MAGNIFICATION FACTOR: $M = \frac{Z_i}{2 Z_o}$

FIGURE 5 SCHEMATIC OF THE SCREEN LENS

This manual system worked very well for printing arrays of holes; excellent arrays on 6.35-μm centers ($2.5 \times 10^6/cm^2$) have been formed using this technique. Figure 6 is a scanning electron micrograph (SEM) of such an array made with a four-exposure step and repeat process. The SEM was taken at an angle of 45° to the surface, so the spacing between the holes is distorted in one direction; however, it is clear from the SEM that the positioning of the holes is very good.

While the manual positioning of the screen/target stage worked very well for printing hole patterns with the screen lens, it would not be possible to traverse the stage manually at a uniform rate to print arrays of lines on the target. To do this obviously requires a controlled motor drive. Stepper motors and associated electronics were purchased and adapted to the screen lens stage drive. The initial set up utilized a manual multiaxis switch interface to address the motors. (Microprocessor interfacing is also available as an add-on.) Figure 7 is a block diagram of the drive system. (System parameters are given in Table 4.) Figure 8 shows the pattern that we planned to lithograph using a 2000-mesh screen and traversing the stage an equal distance in the X and Y directions simultaneously. Figure 9 is a light micrograph of the pattern formed in this way in PMMA resist. The pattern contains 5000 lines, each 10-μm long and about 1-μm wide, in an area 1-mm in diameter. The exposure took about 320 seconds; 25 separate arrays were lithographed simultaneously on a 1/2-inch square substrate.

Figure 10 is an SEM of a portion of a 5000-slot array that has been etched into the molybdenum gate film and the silicon dioxide layer of a cathode structure using the screen-lens exposure scheme described above.

The next phase of the wedge development will entail developing the technology of forming wedges in the slots. This work is scheduled for the next phase of the development program.

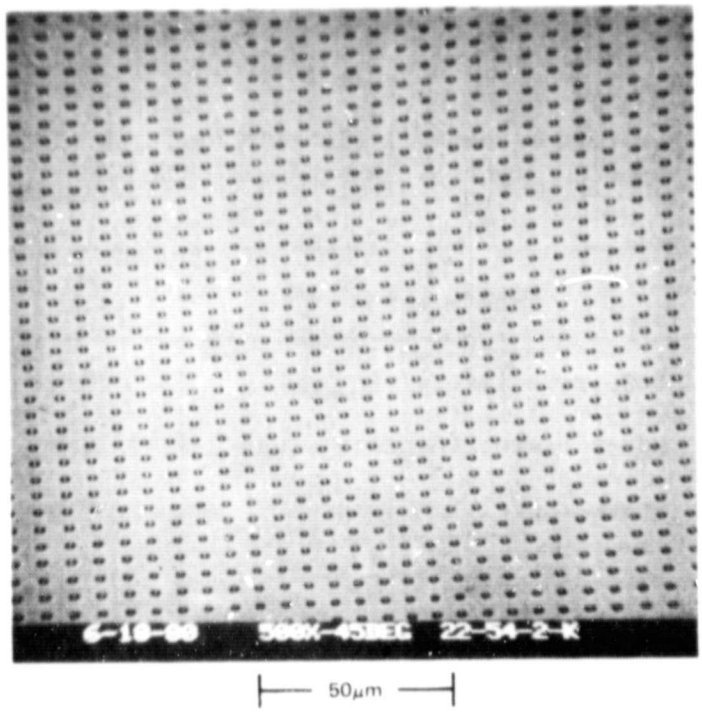

FIGURE 6 PORTION OF A 20,000-TIP ARRAY SPACED ON 0.00025-INCH CENTERS OVER AN AREA 0.040-INCHES IN DIAMETER

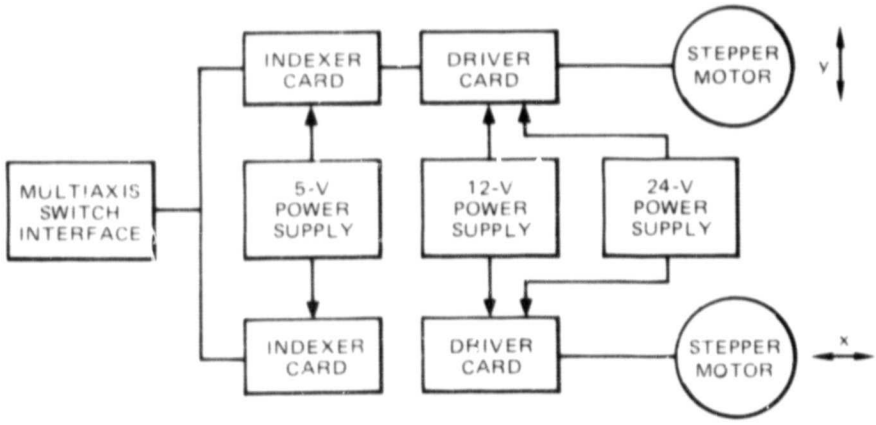

FIGURE 7 STEPPER-MOTOR-DRIVE SYSTEM FOR THE SCREEN-LENS ELECTRON-BEAM LITHOGRAPHY SYSTEM

Table 4

OPERATING PARAMETERS FOR LITHOGRAPHING LINE ARRAYS USING A 2000-MESH SCREEN LENS

Parameter	Value
Step rate (steps/s)	20
Motor travel (degrees/step)	0.9
Stage travel (μm/step)	0.8
Beam spot travel (Å/step)	11
Stage rate (μm/s)	16
Spot rate (Å/s)	220
Spot diameter (μm)	1

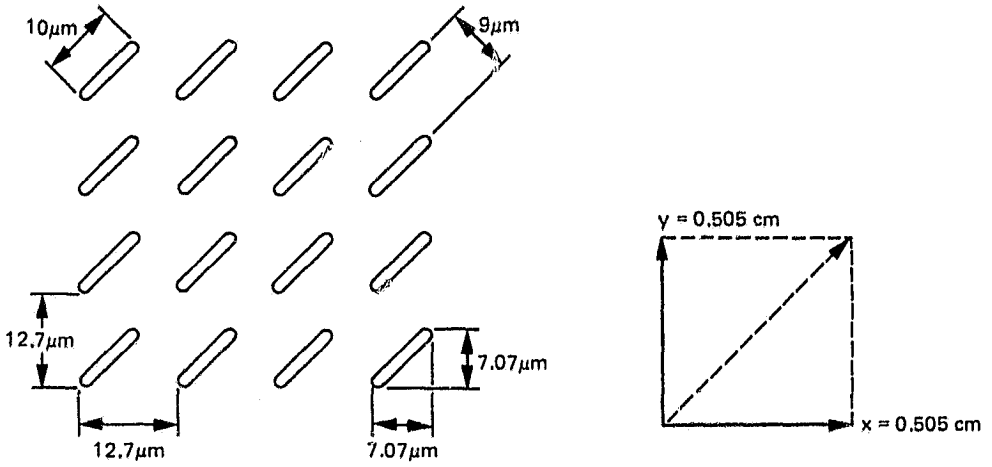

FIGURE 8 PATTERN FORMED USING A 2000-MESH SCREEN LENS AND DRIVING x AND y SIMULTANEOUSLY AT 15.7μm/s FOR 321 SECONDS

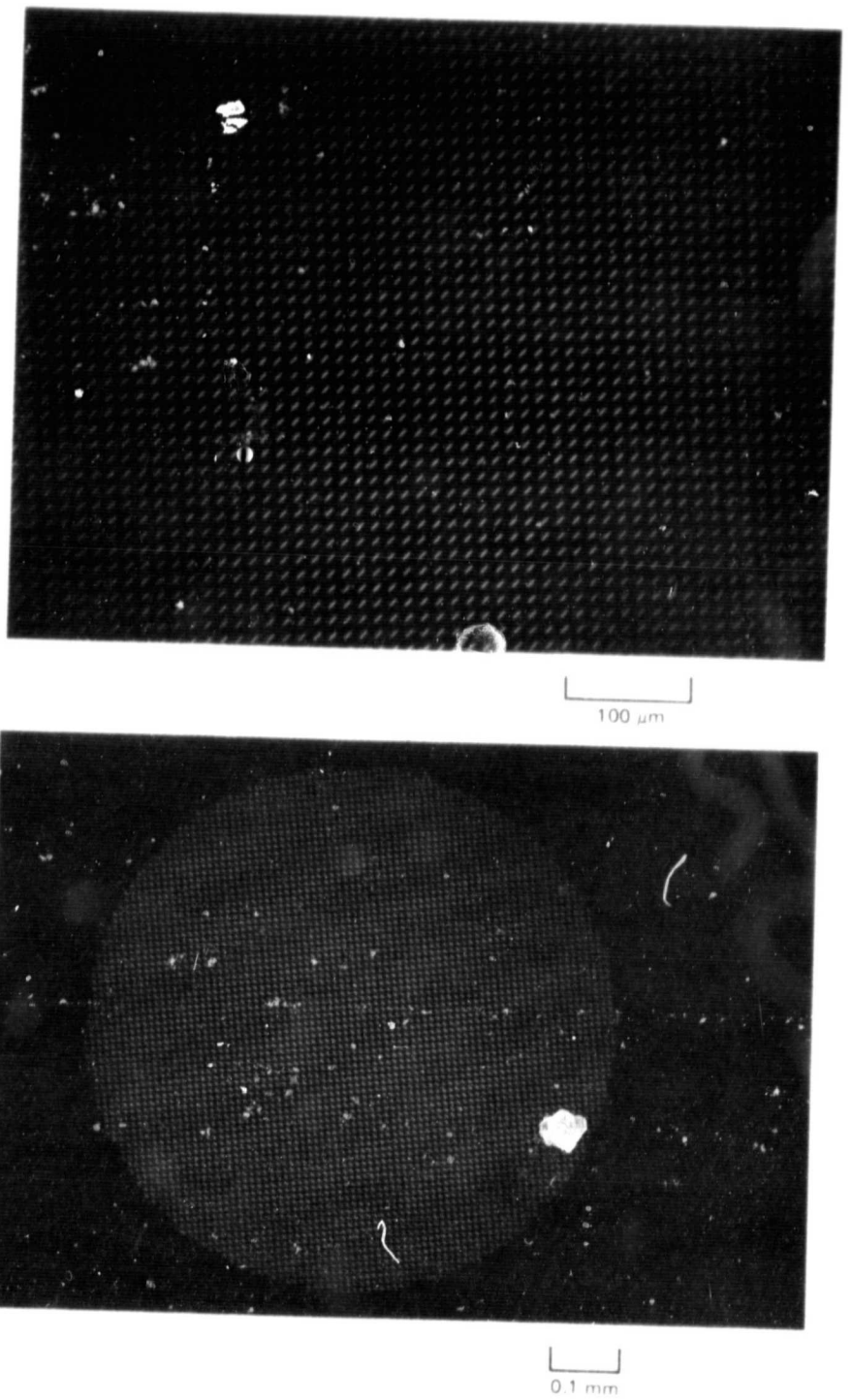

FIGURE 9 LIGHT MICROGRAPHS OF THE LINE ARRAYS FORMED IN PMMA WITH THE SCREEN LENS SYSTEM (5000 LINES IN A 1-mm DIAMETER ARRAY)

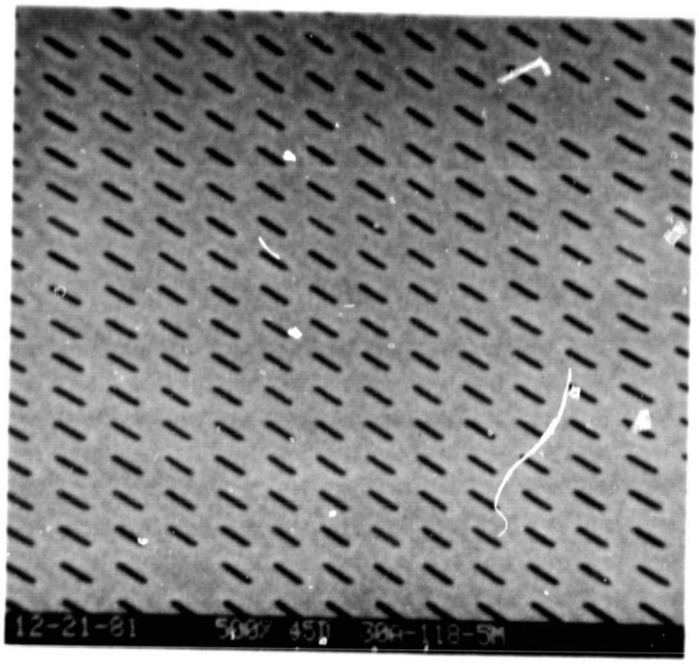

(a) PORTION OF A 5000-SLOT ARRAY (X500)

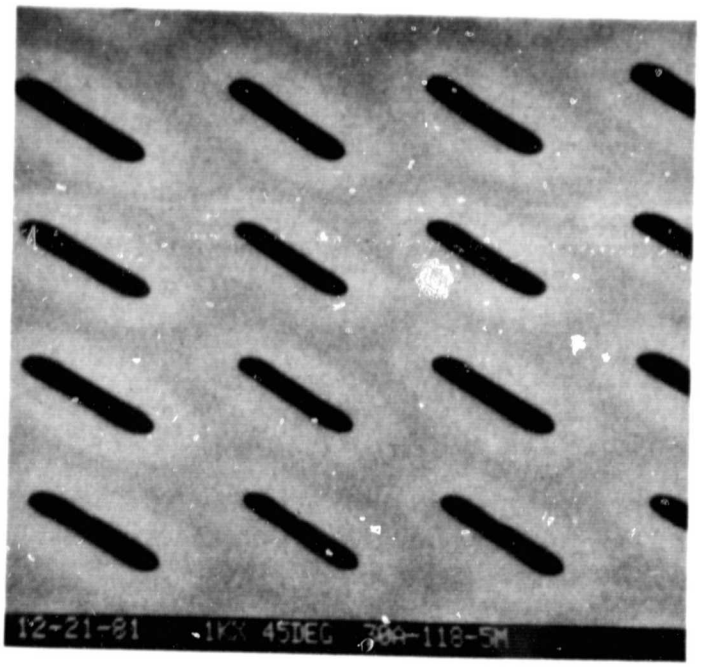

(b) PORTION OF A 5000-SLOT ARRAY (X1000)

FIGURE 10 ELECTRON MICROGRAPH OF SLOTS ETCHED IN MOLYBDENUM GATE AND SiO_2 INSULATING LAYERS

9 μm between rows of lines.

V EMISSION TESTS

A. Initial Emission Tests

All cathodes are tested as they complete the fabrication process, with the exception of cathodes that are obviously not worth testing because of some visible fault, and those that the client requested that SRI deliver untested. The results of these tests are tabulated in the Appendix. All cathodes that were tested are listed, including those on other programs, to give as large a data base as possible. The cathodes are listed by test group. The listing includes bakeout temperature, cathode mount, gate current, applied voltage, maximum emission, number of tips blown during the test, number of shorts between the base and gate during the test, and final condition of the cathode, i.e. OK or NG (no good).

The circuit used for the initial tests is shown in Figure 11. It consists of a simple power supply that delivers a 60-Hz half-wave rectified output that is continuously variable between 0 and -500 V peak; a duty-cycle-control gating circuit that is used to operate the cathode at reduced duty cycle to prevent overheating the collector when operating at emission currents above about 10 mA; and a variable series padding resistor to prevent excessive emission bursts when the cathode is initially turned on.

The cathode tips are driven to a negative voltage by the power supply, and the gate film is grounded. A collector is biased to about +1200 V with respect to ground to help in overcoming space-charge effects in the emitted beam. The collector is a 316 stainless-steel tube, 3/16 inch in diameter and about 1-1/2 inches long. The tube is bent in a gentle curve as shown in Figure 11, and the emitted electron beam is directed into one open end of the tube. In this way the landing impact area is spread out to reduce the power density at the collector, and the tube acts as a Faraday cage to minimize errors due to secondary electron emission. The tube is open at both ends to pump out any desorbed gases.

The emission process is monitored with a dual trace oscilloscope, as shown in Figure 11. The voltage applied to the emitter tips is used to drive the horizontal sweep of the oscilloscope through a 100:1 voltage divider; the gate current is monitored by channel B of the oscilloscope; and the emission current is meaured with channel A. Thus, the applied voltage, the emission current, and the gate current are all monitored simultaneously and can be observed at a glance.

At SRI, three test sites, each of which have positioning for six cathodes, can be operated simultaneously. Thus we can test as many

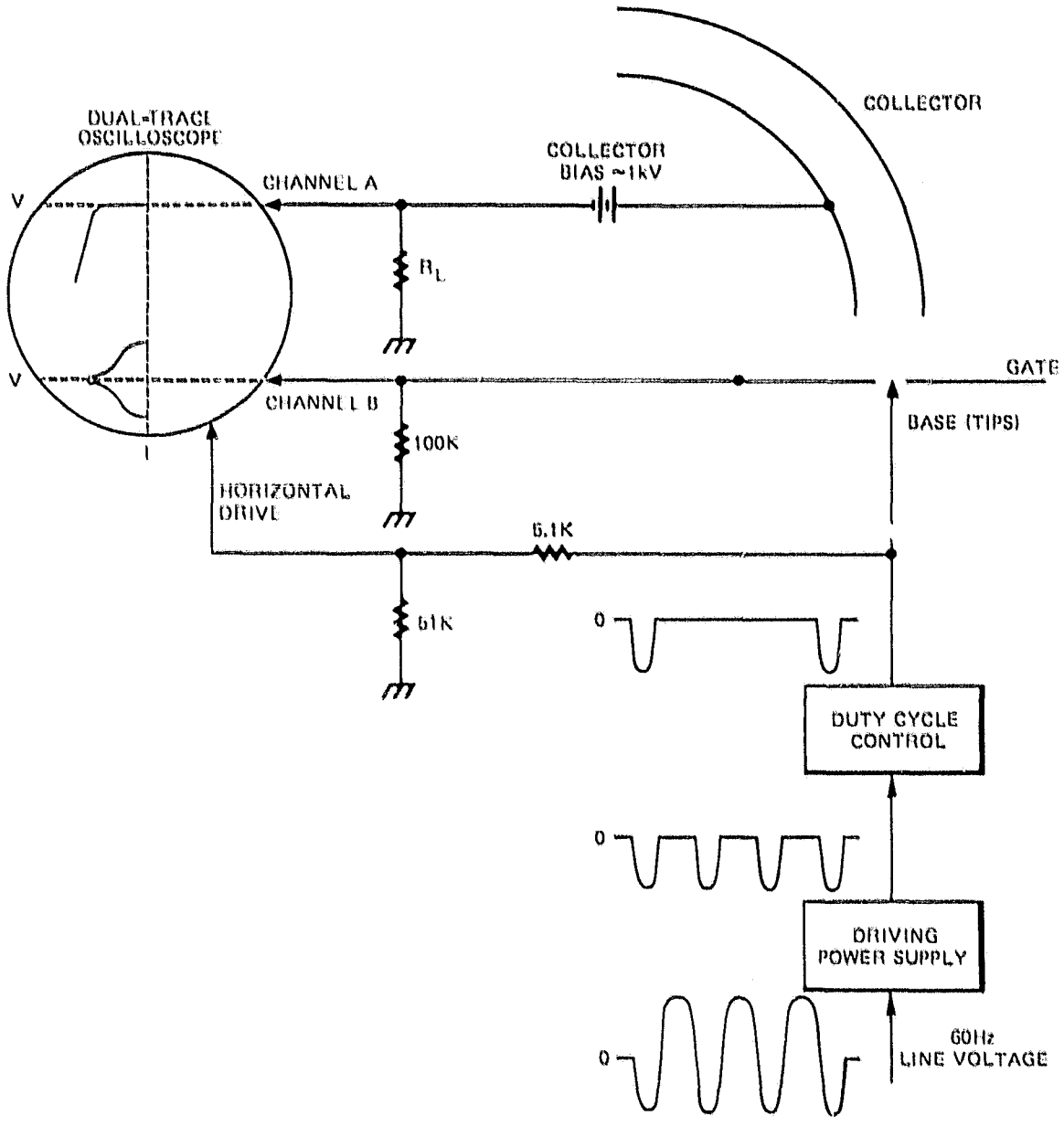

FIGURE 11 SCHEMATIC OF STANDARD EMISSION TEST SETUP

as 18 cathodes at a time. (Usually only 12 are tested at a time because of the characteristics of the vacuum systems and the number of power supplies available.)

Under normal conditions the cathodes are taken up to 20-mA peak emission with the duty cycle reduced to one pulse in 10 through the duty cycle control. We have found that operating at levels much over 10 mA with the full 60-Hz driving signal and the usual +1200 V on the collector overheats the collector (and subsequently the cathode by radiation from the hot collector). Collector temperatures to 900°C have been observed, caused by bombardment from the cathode at peak emission levels of about 20 mA and a 60-Hz driving voltage. Interesting effects have been observed under these conditions; emission is greatly enhanced for a given voltage applied to the cathode. This effect has come to be known as "seasoning."

B. The Seasoning Effect

Figure 12 is a modified Fowler-Nordheim plot of the emission performance of a cathode before and after seasoning. Note that at 70 V the emission has increased by about four orders of magnitude. This remarkable change can take place in about 10 minutes and can be controlled by the operator if done carefully. The technique is simply to increase the emission to a critical level, where the collector becomes very hot and in some way causes the emission to rise without increasing the applied voltage. Little is understood about the mechanism, except that the phenomena has been observed only with the stainless-steel uncooled-type collectors. Thus the assumption has been that the collector is getting hot enough to heat the cathode and produce changes in the surface that have an influence on the emission (e.g. work function)--or that the stainless is reaching a temperature that produces evaporation of some of the material in the stainless steel, and this material is condensing on the emitter tips and changing (lowering) of the work function.

As a check on whether temperature alone was the cause [e.g. thermally assisted field emission (TF) was occuring], a cathode (20A-82-1-I) was seasoned and then turned off overnight. The next day, the cathode was checked after having been off for about 21 hours and found to have the same emission characteristic as when it was turned off the previous day shortly after seasoning. The cathode was left off all of the next five days except for a brief period each morning to check its performance. There was no change in the emission characteristic until the third day. This result indicates that the seasoning effect is not a TF mode emission, but is caused by an exceptionally hot cathode or collector over a period of time.

Two cathodes were examined with Auger spectroscopy to see if material had evaporated from the stainless-steel collector onto the cathode surface. One (20A-82-1-J) was the seasoned cathode; the other (20A-82-1-F) was a control that had been tested at the same time as the

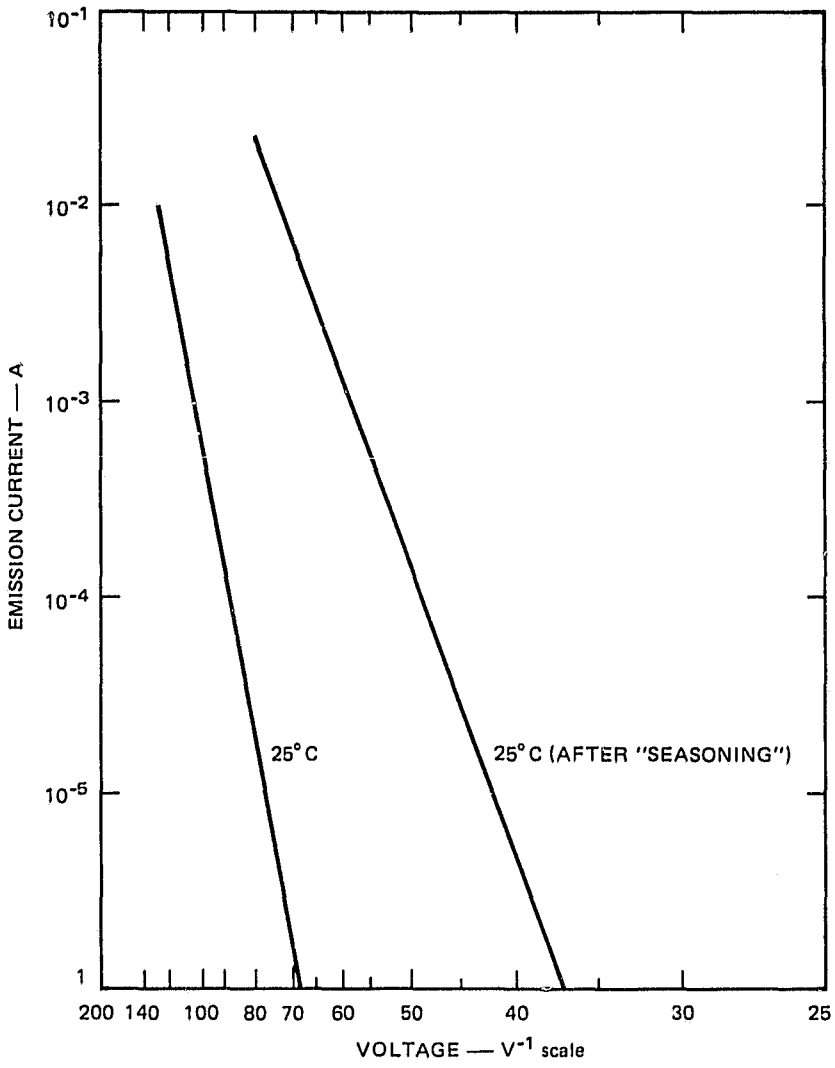

FIGURE 12 CATHODE 20-45-2-X SHOWING EFFECTS OF SEASONING

seasoned cathode, but had not seasoned. Table 5 shows the results. The control showed no evidence of material from the stainless-steel collector, however, the seasoned cathode (20A-81-1-J) contained small amounts of iron, magnanese, chromium, and copper that did not show up on the control sample. All but the copper are materials found in 316 stainless steel, and the copper is probably from a mounting block that supports the stainless-steel collector tube. Clearly the collector was very hot in order to evaporate measurable quantities of these materials onto the cathode. The cathode is only ~3 mm from the collector, and therefore it too must have been very hot. Another notable feature of the data is the relatively large amount of subsurface carbon found on the seasoned (20A-82-1-J) sample. This carbon signal in the spectra of the seasoned cathode was similar in shape to that of a carbide, and the sensitivity of carbide signals can differ by as much as a factor of two from "normal" carbon. Thus, these values for carbon should be taken as high by as much as a factor of two. However, there is no escaping the trend toward high subsurface carbon (carbide) in the seasoned sample. Where the carbon came from is puzzling at this point.

The cathode temperature may also be an important factor. As mentioned earlier, the cathode is very close to the collector (~3mm) and therefore will be heated by radiation. This heating may cause desorption

Table 5

DATA OBTAINED BY AUGER SPECTOMETRY
ON A SEASONED CATHODE AND AN UNSEASONED CONTROL
(DEPTH PROFILE OBTAINED BY SPUTTER ETCHING)

Sample Name/ Etch Depth (Å)	Element (Percent)											
	Si	Na	Cu	Fe	Mn	Cr	O	N	Ca	C	K	Mo
20A-82-1-F (Control)												
0	5.4	0.8	--	--	--	--	47	5.3	--	18	4.9	19
50	2.3	--	--	--	--	--	25	2.4	--	9	1.3	60
20A-81-1-J (Seasoned)												
0	--	0.7	1	1.1	4.1	1.6	51	1.5	--	15	11	12
25	1.6	--	0.4	1.0	2.7	1.9	22	3.7	--	31	1	34
50	1.4	--	--	0.7	2.3	0.4	17	3.1	--	32	--	44
100	2.2	--	--	--	0.9	--	12	1.8	--	26	--	57

of material from the cathode, which results in a net lowering of the work function and thus higher emission levels for a given applied voltage. The desorption of oxygen, for example, could be expected to do this, because oxygen has been shown to lower the emission level for a given applied voltage (Spindt, 1981).

In an effort to begin finding answers to some of the questions raised by these results, SRI conducted an experiment with small evaporators built into four stainless-steel collector tubes. The evaporators were small coils of tungsten wire resistively heated. Two contained 316 stainless steel and two contained gold charges for comparison. The charges were premelted in vacuum for outgassing; the cathodes were then placed in their usual position with respect to the collectors as shown in Figure 13. The cathodes and collectors were processed with SRI's standard pumpdown procedures and checked for the emission threshold by increasing applied voltage until the onset of emission.

Results with the gold deposition onto cathode 20A-110-2-U were as follows: The system was baked at 400°C for 85 hours and then cooled for 5 hours. Voltage was applied to the collector and cathode, and the emission was brought up to 10 μA. The emission was very stable, and the voltage required to maintain 10 μA decreased overnight from 106 V to 89 V.

Current was then applied to the gold evaporator and increased slowly. When the heater current to the evaporator reached 2 A the emission began to fall off (with the applied voltage held at 89 V). The emission dropped to 6 μA and stabilized. After 5 minutes at 6 μA, the heater current was increased to 2.1 A, and the emission began to climb back toward 10 μA. After 5 minutes it had surpassed 10 μA and was continuing to increase. In an additional 5 minutes the emission was up to 20 μA. The evaporator heater current was then turned off; the emission dropped off to 10 μA in few minutes, and was then stable at 10 μA. After being off for 10 minutes, the evaporator heater was turned on again and brought up to 2.1 A for 3 minutes and then 2.2 A for 15 minutes. There was no change in emission during the first 3 minutes, but during the 15 minutes at 2.2 A the emission increased to 32 μA, and the first sign of gate current appeared in the form of leakage between the base and gate. The evaporator current was turned off again; the emission stabilized at 32 μA, and the gate current stabilized at 10 μA of leakage current. After one hour of unchanging emission and gate current, the evaporator heater was again turned on and the current set at 2.2 A. The gate current increased to 14 μA and then became erratic. The evaporator was turned off again, and the gate wandered from 20 μA to 32 μA and finally back to 10 μA after about 7 hours. During this time the emission went from 30 μA to 20 μA and back to 30 μA in a slow drift. No further gold deposition was attempted on the assumption that some tips had blown out, and that the gold would therefore cause a conductive path between the base and gate (gate current) because the protective gate overhang in the holes would be removed by any blowouts. A subsequent inspection showed that several tips had indeed blown out.

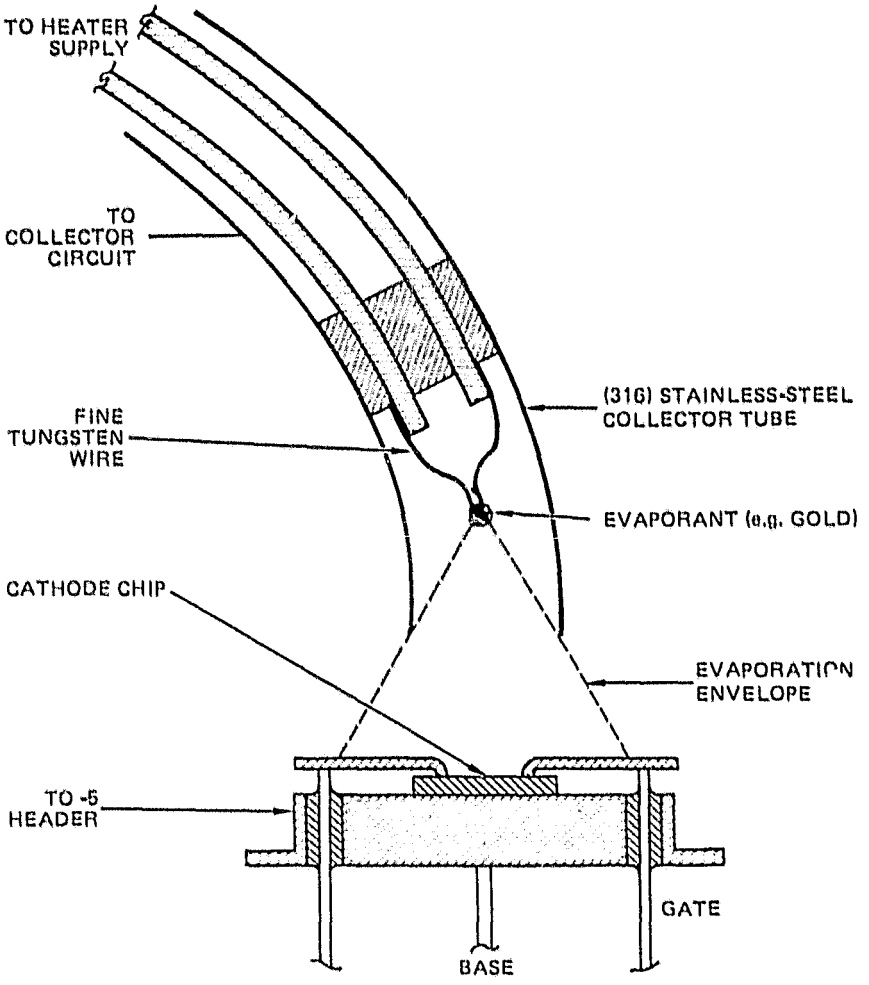

FIGURE 13 SCHEMATIC OF THE EVAPORATOR APPARATUS USED TO COAT CATHODE ARRAYS IN SITU

During emission measurements, evaporator is common with the collector tube.

A similar test was done with the 316 stainless-steel evaporator on cathode 20A-107-7. Low-level emission was established to mimimize the chance for blowing out any tips, and the evaporator heater was turned on. The emission was 0.1 μA at 80 V when the evaporator was turned on. The evaporator temperature was increased gradually, and the emission increased slowly for 20 minutes to 1.8 μA and then slowly fell to 0.4 μA over the next 20 minutes. The evaporator was then turned off, and after an additional hour the emission was down to 0.2 μA. The cathode was then turned off. Subsequent examination showed obvious deposition on the cathode and one tip blown.

In summary, the gold deposition increased the emission by a factor of three and caused excessive gate current. The 316 stainless-steel evaporation caused an increase in emission by a factor of 10, but with additional evaporation the emission reversed itself and fell back to the (original) value observed before deposition onto the cathode. In neither case did the observed values approach the four-orders-of-magnitude change that was measured with cathodes that were seasoned by heating the collector to high (~900°C) temperature with the emission current from the cathode.

The next step is to test a cathode under high temperature conditions to see if high temperature is causing a surface charge, e.g. by desorption, that can account for the large emission enhancement that has been observed. For example, if some contaminant such as oxygen is on the surface and produces a surface with a work function of 5.5 eV, desorption of this contaminant would lower the work function to that of clean molybdenum, or about 4.5 eV. With a field of 2×10^7 V/cm, this would cause an increase in the current of about five orders of magnitude (Dyke and Dolan, 1956).

Another possibility is that the stainless steel, the temperature, and the fields all interact to produce the effect. Whatever the cause, the results produced to date indicate that the deposition of stainless steel onto the surface does not by itself produce the dramatic increase in emission current that has been observed with the seasoning effect.

C. Tests with a Commercially Processed Tube

An important question regarding use of the field emitter cathode is whether it can be operated in a "real tube" environment or whether special tube processing will be required to use the cathode in traveling wave tubes. In order to investigate this question, NASA contracted with the Watkins-Johnson Company to obtain a "real" tube for testing the cathode, and then requested SRI to provide Watkins-Johnson with cathodes and consultation on their testing prior to shipment of the tubes to NASA.

A tube to use as a test vehicle was assembled by Watkins-Johnson using a NASA gun design. The tube, shown in Figure 14, has no helix

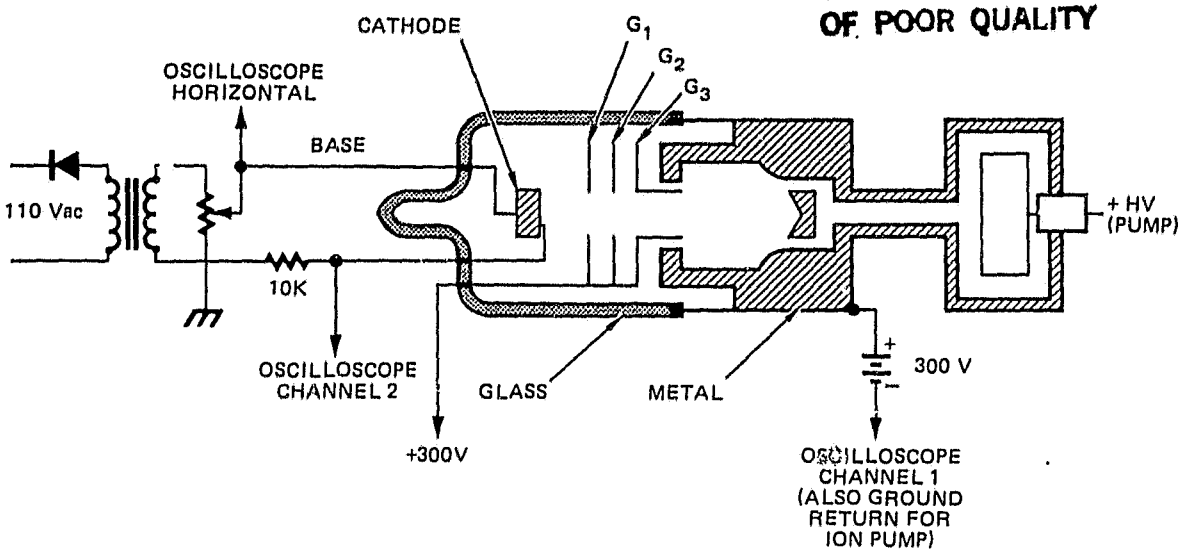

FIGURE 14 SCHEMATIC OF TEST CIRCUIT FOR TESTING WATKINS-JOHNSON TUBE UP TO 1mA AT 300V BY FLOATING TUBE BODY

structure; a periodic structure is not needed to check cathode performance, and would be an unneccessary added expense.

The tube consisted of a cathode mount, a three-element molybdenum lens structure mounted on sapphire rods, and a copper collector. The gun section had a 1/2-inch-diameter glass envelope, and the collector section had a 1-1/4-inch diameter metal (copper) envelope. A holding pump was mounted on the collector section as shown. All of the materials and processes used were standard Watkins-Johnson procedure.

A cathode (20A-107-7-L) was pretested at SRI and delivered to Watkins-Johnson for mounting in the gun structure and for assembly of the gun and tube. The assembled tube was evacuated with an 80-liter/s ion pump and baked at 400°C for 15 hours while pumping. Pressure at the pump was in the 10^{-10} torr range when the tube was pinched off.* The tube was then stored for several days with the pump off while testing facilities at Watkins-Johnson were arranged. Voltage was then applied to the pump, and a definite surge in current was noted, indicating that the pump started. The pump current subsided quickly as the gasses that evolved during the starting pressure burst were repumped.

Gun electrodes G_1, G_2, and G_3 (Figure 14) were connected to the collector, which was biased to +300 V as shown. The cathode drive for the first turn-on was the same as used at SRI to pretest the cathodes, i.e. a 60-Hz half-wave rectified driving voltage. The driving circuit is also shown in Figure 14.

---

*All of this is standard Watkins-Johnson tube-processing technique.

The total emission current was raised to a level of 1 mA peak over a period of 7 days and was very stable during the entire time. It had been agreed that although the cathode had been operated up to 20-mA peak emission in SRI's initial tests, we would not exceed 1 mA in the tube; we would demonstrate only that it was working properly and then ship it to NASA for further testing. The cathode required 175 V to produce 1-mA emission in the tube. This compares very well with the initial test at SRI which required 180 V to produce 1 mA. If there was any real difference it was in the favor of the Watkins-Johnson tube environment.

The tube was designed to operate in a 2-kG axial B field to keep the beam from diverging. In order to determine the extent of the divergence, the distribution of the emission current between the electrodes in the tube was measured with the B field on and off. The results are shown in Table 6. They show that with the B field on, 1 mA reached the collector and only 15 μA was measured on the gun electrodes when all the electrodes were at +300 V, the gate was at ground, and the tips were -175 V. Without the B field, the emission current was divided equally between the collector and gun electrodes (0.5 mA each).

Table 6

CURRENT DISTRIBUTION AMONG THE WATKINS-JOHNSON TUBE ELECTRODES WITH THE B FIELD ON AND OFF
(See Figure 14)

Configuration*	Drive Voltage (V)	Gate Current (μA)	Collector Current (mA)	G_1 Current (μA)	$G_2 + G_3$ Current (μA)
B Field On	170	70	1	10	5
B Field Off	170	20	0.5	200	300

*$G_1 = G_2 = G_3 = V_{COL} = +300$ V

The gate current was higher than expected at 70 μA when the magnetic field was on. Unexpectedly, the gate current dropped to 20 μA with the magnetic field off and everything else the same. This suggests that the observed gate current was due to something other than intercepted emission current. The cathode had no gate current at all at

1-mA emission levels during the preliminary tests at SRI, so it is possible that the apparent gate current was due to some interelectrode emission not involving the active area of the cathode itself.

The emission current was well behaved and stable throughout the test, indicating that the vacuum environment in tubes as processed at Watkins-Johnson is compatible with the requirements of the field emitter array.

The tube was shipped to NASA for additional testing, however, these tests were not completed because of arc damage to the cathode. The damage occurred before the cathode was turned on, so it may have been the result of a discharge when the pump was started after having been off during shipping.

D. Failure Analysis

A variety of failure modes have been observed during the cathode-testing experiments. Failure of a cathode is almost always due to an electrical short between the base and gate. In rare cases, the voltage required to maintain emission increases during operation to such an extent that the cathode becomes essentially inoperative.

Failures often occur in groups of cathodes, indicating a fabrication fault built into that group. Usually the fault is in the form of surface contamination, the result of a slip in the processing procedure. For example, we have observed stains with a "water spot" appearance and traced the problem to a contaminated cathode-holding-tool handle. The handle was touched by a worker from another project who didn't realize the problem that this would create, and the cathode technician was unaware of the event. The result was that when the tool was used to transport the cathode into solvents during the final cleaning, the solvent vapors washed the contamination from the tool handle into the final rinses. Then, when the cathode was dried in hot nitrogen, the contaminant was left behind in the form of spots on the cathode surface.

Cathodes that have been tested with visible spot-like stains almost always suffer electrical breakdown in the areas of the spots. This kind of breakdown usually occurs at advanced emission levels, e.g., ~1 mA of emission. This gives the impression that as the cathode is warmed by heat from the collector and reflected primaries strike the gate surface in significant numbers, the contaminant volatizes, creating a local high pressure that causes an electrical discharge.

We have learned to recognize this kind of contamination on the cathodes, and have investigated ways of removing it. Through these efforts we have learned that this general type of contamination is remarkably robust, and we have been unable to completely eliminate it except by sputtering. Unfortunately, sputtering also shorts out the cathode by sputturing molybdenum from the sides of the cones onto the silicon-dioxide walls of the holes. The best way to fix this problem

is to avoid the contamination in the first place, and we are therefore taking great care with our processing procedures, with a noticeable improvement in our results.

Other fabrication faults that have caused trouble are overetching of the oxide layer and incomplete removal of photoresists. Overetching the oxide produces a large area of unsupported molybdenum gate film around the hole that is susceptible to cracking during processing--especially during ultrasonic cleaning--and possibly to overheating during operation if there should be any intercepted emission. Photoresist residue produces the same result as the contamination discussed earlier. That is, the residue produces gases that lead to electrical discharges and breakdown of the sandwich structure.

These contamination-caused failures usually produce many individual tip failures that eventually reduce the cathode's performance to a substandard level. Occasionally the gas pressure gets high enough to produce a discharge between the cathode and collector; when this happens the damage is usually severe enough to short the cathode's base and gate together so that the cathode becomes inoperative.

Other sources of failure have been outgassing from other electrodes, such as collectors, and contamination collected on the cathode during storage and handling. It is obvious that debris and other surface contamination on the cathode should be avoided; however, when handling the cathodes for shipping or mounting it is very difficult to assure that everything is kept absolutely clean. It is apparent that the cathodes should be handled only under clean-room-like conditions, and these conditions are not found in most laboratories.

An examination of cathodes that have been stored for long periods of time in plastic boxes showed that some were unchanged as far as we could tell while others (which were right alongside of the unchanged cathodes) had obvious surface changes that looked like the molybdenum had oxidized. It appears that the molybdenum gate film's ability to resist corrosion depends upon the film's history. Generally, cathodes made a few years ago, when aluminum or gold was commonly deposited over the molybdenum gate film and subsequently etched away, tended to corrode in a relatively short time. In the last few years we have found that most cathodes do not tend to visibly corrode even after being stored in the same environment as the older cathodes for over a year. Thus, it appears that the newer processing produces a molybdenum surface that is relatively corrosion resistant when stored in clean plastic boxes on our laboratory shelf. Cathodes have been retested after storage under these conditions with mixed results, showing that long-term storage at laboratory shelf conditions can, but does not always, degrade the cathode. Table 7 shows the results of two tests on two cathodes from the same group that illustrates this effect. The cathodes were tested side by side in the same vacuum each time and were stored side by side in the same box for 5 months between tests.

Table 7

RESULTS OF TESTS ON TWO CATHODES KEPT SIDE BY SIDE DURING FABRICATION, TESTING, AND STORAGE

Cathode/Test	Bake	Gate Current (μA)	Applied Voltage (V)	Emission (A)	Tips Blown	Shorts	Storage Time (Mo)
20A-114-1-F							
1	400°C	-11	180	10	23	0	0
2	450°C	-20	220	10	17	1	5
20A-114-1-G							
1	400°C	-2	180	10	12	1	0
2	450°C	-4	180	10	0	0	5

Nevertheless, the cathodes behaved differently on the two tests. Obviously more must be done to determine the effects of storage and to establish preferred storage conditions, if necessary.

E. Life Test

A 100-tip cathode array has been operating on life test since 17 March 1975. The cathode was checked at 3-mA peak emission with our standard 60-Hz drive voltage and then set at 2 mA. Over the years the emission has been changed for various reasons (such as equipment failures) but has never been below 2 mA peak. During the last few years the emission has been increased and is now at 5 mA peak. Table 8 shows a summary of the cathode's operation and Figure 15 shows oscillographs of the voltage/current characteristic at the start of the test and recently. The voltage required for a given emission has increased since the cathode was first turned on, but most of this increase occurred early in life and the cathode has been stable for the last several years.

The present level of emission is 5 mA peak with the 60-Hz drive voltage as shown in Figure 15. This is an average emission of 50 μA per tip. The 17 series cathodes contained 100 tips spaced on 25-μm centers, or a packing density of 1.6×10^5 tips/cm^2; thus, the current density for this cathode is 8 A/cm^2 when operating at a total current of 5 mA. Because the operation of each tip should be independent of the other tips, we should expect to realize higher current densities by simply increasing the tip packing density and operating the cathode

Table 8

LIFE TEST HISTORY

Date	Operating Characteristics		Cumulative Operation (hours)
	Applied Voltage (V)	Emission (mA)	
14 March 75	320	2	
2 March 78	350	2	8,500
5 May 79	380	2	18,700
11 June 80	360	2	28,000
21 July 80	360	3	47,000
17 January 82	360	4	60,000
4 February 82	390	5.5	60,400
14 June 82	390	5.5	63,200
11 November 82	390	5.0	66,300

under the conditions that produce 50 μA per tip--a level of emission that we have shown can be sustained for long periods. We have shown that our fabrication technology is capable of producing arrays of tips having packing densities of 2.5×10^6 tips per cm^2 (Figure 6). Then it is probable that these cathodes will produce current densities of 125 A/cm^2 with good lifetimes (50 μA/tip x 2.5×10^6 tips/cm^2). Realizing this potential will depend on our ability to develop an etching technology for the SiO_2 layer that does not undercut the molybdenum gate film to such an extent as to break into the neighboring hole. Plasma etching appears to hold great promise for achieving this goal.

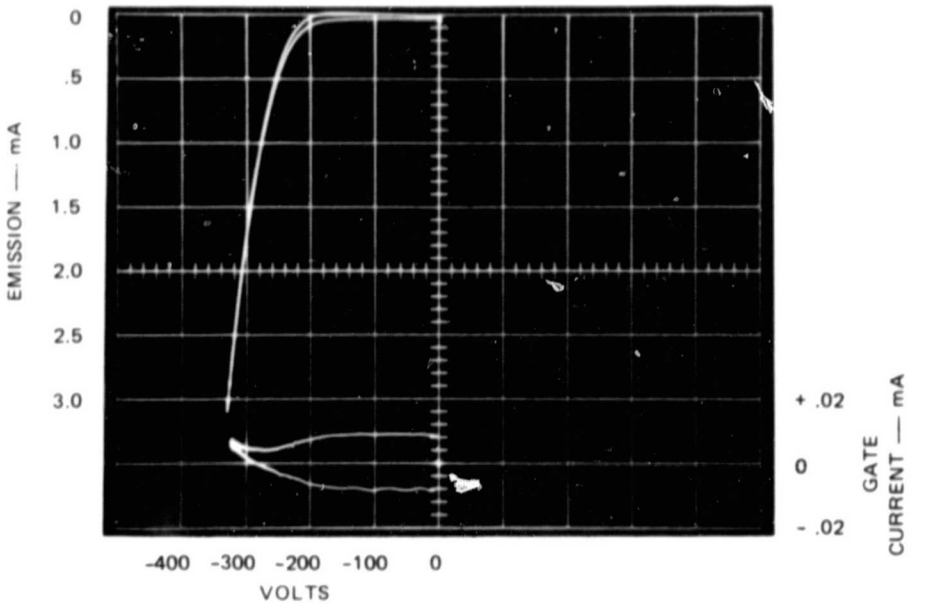

(a) START OF LIFE TEST (MARCH 17, 1975)

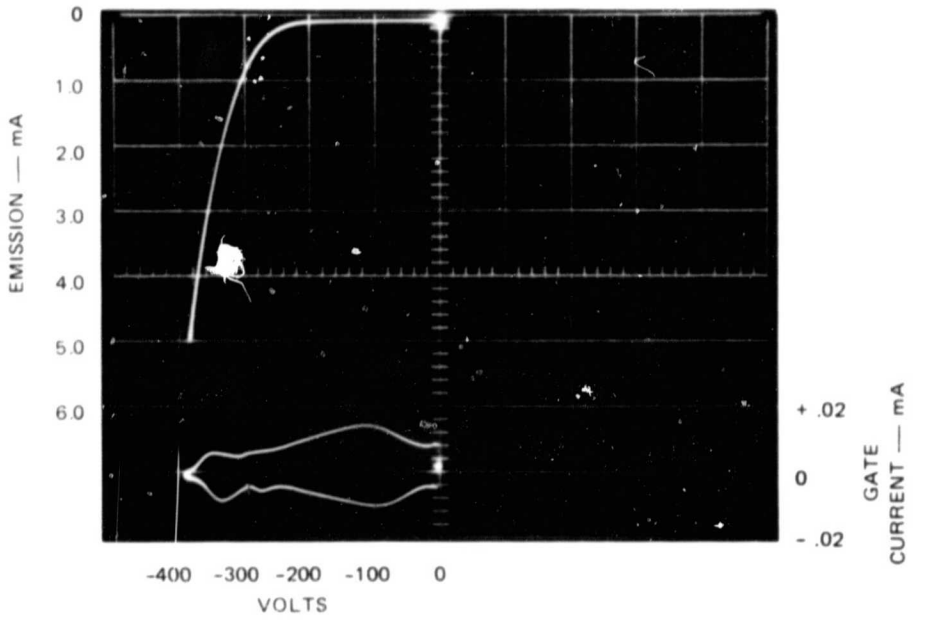

(b) EMISSION AFTER 66,000 HOURS (NOVEMBER, 1982)

FIGURE 15 CURRENT–VOLTAGE OSCILLOGRAPHS FOR 100–CONE ARRAY No. 17–13–17–G DRIVEN BY A 60–Hz HALF–WAVE VOLTAGE TO A PEAK CURRENT OF 3 mA FOR 53,000 HOURS

VI SUMMARY AND CONCLUSIONS

The purpose of this phase of the program was to fabricate, test, and deliver state-of-the-art cathodes to NASA; advance the fabrication technology; study failure mechanisms; and develop the technology for fabricating wedge-shaped cathodes to complement the conventional cone-shaped emitters.

A total of 141 cathodes were pretested. Of these, 113 were the state-of-the-art configuration; however, many of the 113 were experimental, in that new processing technology was being tried (as discussed in Section IV-B). As a result, problems due to photoresist residue and resist breakdown reduced our yield before they were identified and solved. Of the 141 cathodes that were tested, 67 operated at 20-mA or higher emission; 8 additional cathodes were operated at the 10-mA level. A total of 67 cathodes were working after the initial tests. Of the 74 that were not working, 36 suffered from mounting and connector problems or vacuum problems. The remaining 38 failures were primarily due to discharges that shorted the cathode.

A total of 32 cathodes were delivered to NASA and NRL. Of these, 12 were delivered untested; the remaining 20 were pretested at SRI prior to delivery. The results of the tests were shipped with the cathodes.

During this program, many basic fabrication details were modified and improved. These improvements were generally not of the type that is visible in the finished cathode, but they have improved efficiency in fabrication and the performance of the cathode. For example, depositing the gate film over the entire wafer immediately after the oxidation process has greatly improved the integrity of the interface between the oxide layer and the deposited molybdenum gate film. Having the gate film in place during subsequent processing steps also protects the oxide layer. This change required that we develop a good deal of photolithography for various patterning steps on the gate film and active area; these were difficult--primarily because of the necessity to reliably cover holes with photoresist and to completely remove the photoresist after etching without damaging the molybdenum gate or the holes. The final result, however, has been very good, because we now have much more flexibility in the process than was possible with the old technique (using shadow masks during both gate film deposition and electron lithography to pattern our electrodes and active areas respectively.)

The apparatus necessary for fabricating arrays of wedge-shaped cathodes has been completed, and arrays of slots suitable for forming

wedges have been micromachined in silicon/silicon-dioxide/molybdenum sandwich structures with the new system.

Operational tests were done to investigate the feasibility of deliberately seasoning cathodes by evaporating layers onto the emitters in situ. The results indicate that heating the cathodes may be an important factor in the seasoning phenomena, and that desorption of contaminants from the tips (e.g. oxygen) may be the major cause of the effect.

A cathode was mounted in a traveling-wave-like tube gun structure using conventional tube-processing techniques. The cathode operated well in preliminary tests, giving very stable, noise-free emission up to 1 mA (which was as high as it was taken before being shipped to NASA for further tests). The cathode operated for a week without any degradation before being shipped, indicating that the standard tube process vacuum (as done by Watkins-Johnson) is probably adequate for field-emission array operation.

A review of cathode operation with a view toward the causes of cathode failures strongly suggests process faults as a major cause. Those that failed in the initial tests were probably flawed by contaminants (usually resist materials); those that failed later were probably contaminated during handling and storage. Stringent cleanliness must be maintained at all times with the cathodes.

A life test has been in progress for over seven years with the cathode operating at an average tip loading of 20 μA per tip or higher during the first seven years and at 55 μA per tip for the last $8{,}000_5$ hours. The cathode under test has a tip packing density of 1.6×10^5 tips/cm, and this is operating at 8.8 A/cm^2. Cathodes currently being produced have 6.4×10^5 and 1.2×10^6 tips/cm^2, and would produce 35.2 A/cm^2 and 70.4 A/cm^2, respectively, under the same tip loading.

REFERENCES

Brodie, I., 1975: "Bombardment of Field-Emission Cathodes by Positive Ions Formed in the Interelectrode Region," Int'l J. of Electronics, Vol. 38, 4, pp. 541-550 (April).

Burges, R.B., H. Kroemer, and J.M. Houston, 1953: "Corrected Values of Fowler-Nordheim Field Emission Functions v(y) and s(y)," Phys. Rev., Vol. 90, 4, pp. 173-181 (1 May).

Dyke, W.P., and W.W. Dolan, 1956: Advances in Electronics and Electron Physics, Vol. 8, p. 98 (Academic Press, New York, New York).

Fowler, R.H., and L.W. Nordheim, 1928: "Electron Emission in Intense Electric Fields," Proc. Royal Soc. (London), Vol. A119, p. 173-181 (1 May).

Heynick, L., Westerberg, E.R., Hartelius, C.C., and Lee, R.E., 1975: "Projection Electron Lithography Using Projection Lenses," IEEE Trans. on Electron Devices, ED-22, 7, p. 399 (July).

Spindt, C.A., 1980: "Development Program on a Cold Cathode Electron Gun," NASA Report CR-15866, SRI Project 7906, prepared by SRI International, Menlo Park, California 94025.

Spindt, C.A., 1981: "Development Program on a Cold Cathode Electron Gun," NASA Report CR-165401, SRI Project 1074, prepared by SRI International, Menlo Park, California 94025.

Spindt, C.A., Brodie., I., Humphrey, L., and Westerberg, E.R., 1976: "Physical Properties of Thin Film Emission Cathodes," J. Appl. Phys., Vol. 47, No. 12, p. 5248 (December).

Appendix

CATHODES TESTED IN THIS PHASE OF THE RESEARCH PROGRAM

Cathode	Mount	Bake Temp (°C)	Current Gate (mA)	Applied Voltage (V)	Emission (mA)	Tips Blown	Shorts	Notes
Group 1								
20A-82-1-F	TO-5	400	0.035	155	≧	>100	1	NG*
-I	TO-5	400	5.5	80	20	~1000	0	Seasoned; OK
-J	TO-5	400	5	70	20	~100	1	Seasoned; OK
-B	TO-5	400	0.004	190	20	~150	0	OK
-C	TO-5	400	0.006	160	10	>100	0	NG; ARC
-D	TO-5	400	0.03	190	10	>100	0	NG; ARC
Group 2								
(no cathode)								
25A-84-3-B	Al_2O_3	400	0	290	0.01	All	0	NG; ARC
-C	Al_2O_3	400	0	300	0.05	0	0	NG; high voltage
-F	Al_2O_3	400	0.005	300	0.06	0	0	NG; high voltage
-G	Al_2O_3	400	0	330	3	0	0	OK
-H	Al_2O_3	400	0	355	0.005	All	0	NG
Group 3								
20A-82-1-H	TO-5	380	--	--	--	--	--	No contact
-N	TO-5	380	0.04	200	10	~500	0	OK
-O	TO-5	380	0	222	2	35	0	OK; power supply problem
-P	TO-5	380	--	--	--	--	--	NG; mount shorted
-Q	TO-5	380	0	140	0.002	~100	0	OK; power supply problem
-T	--	--	--	--	--	--	--	No contact
Group 4								
20A-82-3-C	To-5	400	0	200	10	25	0	OK
-D	TO-5	400	0.002	200	10	8	0	OK
-B	TO-5	400	0.12	200	10	~500	5	OK;. mechanical damage
-F	TO-5	400	--	--	--	--	--	No contact
-R	TO-5	400	--	--	--	--	--	No contact
(No cathode)								

*No good

Cathode	Mount	Bake Temp (°C)	Current Gate (mA)	Applied Voltage (V)	Emission (mA)	Tips Blown	Shorts	Notes
Group 5								
23A-68-3-B	TO-5	370	0	150	1	2	2	OK
-C	TO-5	370	--	--	--	--	--	No contact
-D	TO-5	370	--	--	--	--	--	No contact
-F	TO-5	370	0	180	1	21	8	NG; ARC
-G	TO-5	370	0.002	145	1	1	2	OK
(No cathode)								
Group 6								
20A-71-3-P	TO-5	390	0.019	200	3.5	~100	1	NG; vacuum leak
20A-82-2-F	TO-5	390	0	200	1	~200	2	NG; vacuum leak
-G	TO-5	390	0	170	1	~100	1	NG; vacuum leak
-I	TO-5	390	0	155	1	~200	7	NG; vacuum leak
-L	TO-5	390	0	210	1	~200	1	NG; vacuum leak
-M	TO-5	390	0	168	1	~100	4	NG; vacuum leak
Group 7								
23A-99-2-B	Al_2O_3	380	0.004	220	0.25	30	0	NG
-C	Al_2O_3	380	0.007	270	0.25	56	0	NG
-D	Al_2O_3	380	0.002	210	0.25	31	0	NG
-F	Al_2O_3	380	0	200	0.25	15	0	NG
-G	Al_2O_3	380	0	210	0.25	24	2	NG
-H	Al_2O_3	380	0	215	0.25	20	1	NG
Group 8								
23A-99-3-B	Al_2O_3	400	0	218	0.1	15	1	NG
-C	Al_2O_3	400	0	210	0.1	1	0	OK
-D	Al_2O_3	400	0	230	0.1	0	0	OK
-E	Al_2O_3	400	0	220	0.1	0	0	OK
-F	Al_2O_3	400	0	300	0.1	0	0	OK
-G	Al_2O_3	400	0	265	0.1	5	1	OK; poor

Cathode	Mount	Bake Temp (°C)	Current Gate (mA)	Applied Voltage (V)	Emission (mA)	Tips Blown	Shorts	Notes
Group 9								
20A-79-1-F	TO-5	390	0.03	295	0.5	>100	0	NG; vacuum leak
-P	TO-5	390	—	—	—	—	1	NG; vacuum leak
-R	TO-5	390	—	—	—	—	2	NG; vacuum leak
-V	TO-5	390	—	—	—	—	—	No contact
-W	TO-5	390	—	—	—	—	—	No contact
-X	TO-5	390	—	—	—	—	—	No contact
Group 10								
20A-107-7-B	TO-5	400	0.1	186	21	~1000	1	NG; vacuum leak
-C	TO-5	400	0.035	172	22	~700	1	OK; vacuum leak
-D	TO-5	400	—	—	—	ARC	1	NG; vacuum leak
-F	TO-5	400	0.33	195	50	~2000	1	NG; vacuum leak
-G	TO-5	400	0.1	190	21	~1000	1	NG; vacuum leak
-H	TO-5	400	0	200	0	14	2	NG; vacuum leak
Group 11								
20A-82-2-B	TO-5	400	0.02	92	20	70	0	OK; seasoned
-N	TO-5	400	0	184	20	—	2	OK
-O	TO-5	400	—	—	—	—	1	NG; ARC
-P	TO-5	400	0.01	205	25	—	2	OK
-Q	TO-5	400	0.008	200	20	—	0	OK
-S	TO-5	400	—	—	—	—	1	NG; ARC
Group 12								
20A-107-7-I	Al_2O_3	390	0.018	180	25	47	0	OK
-J	Al_2O_3	390	0.021	200	25	13	0	OK
-L	Al_2O_3	390	0.025	220	28	3	0	OK
-M	Al_2O_3	390	—	—	—	—	—	No contact
-N	Al_2O_3	390	0.05	220	15	40	0	OK
-O	Al_2O_3	390	0.042	189	112	4	0	OK

Cathode	Mount	Bake Temp (°C)	Current Gate (mA)	Applied Voltage (V)	Emission (mA)	Tips Blown	Shorts	Notes
Group 13								
20A-70-1-J	TO-5	380	0.02	185	40	~500	2	OK
-Q	TO-5	380	1.0	120	60	60	0	OK; seasoned
-V	TO-5	380	0	170	20	6	0	OK
-W	TO-5	380	2.4	67	25	65	0	OK; seasoned
-Y	TO-5	380	4.2	58	20	—	0	OK; seasoned
-B	TO-5	380	1.3	125	70	—	1	NG; ARC; seasoned
Group 14								
20A-70-2-C	TO-5	380	0.025	145	100	~75	5	OK; partially seasoned
20A-81-3-B	TO-5	380	—	--	--	--	--	No contact
-C	TO-5	380	0.004	178	65	~100	2	OK; cracked
-D	TO-5	380	0.9	190	2	~2000	3	NG; cracked
-F	TO-5	380	—	--	--	--	--	No contact
-G	TO-5	380	—	--	--	--	--	No contact
Group 15								
20A-110-2-N	Al_2O_3	380	10	230	10	12	1	NG
-P	Al_2O_3	380	0	210	8	19	2	NG
-Q	Al_2O_3	380	0.170	245	20	9	0	OK
-M	Al_2O_3	380	--	--	--	—	--	No contact
-R	Al_2O_3	380	0.041	235	22	1	0	OK
-K	Al_2O_3	380	—	--	--	—	--	No contact
Group 16								
20A-112-5-B	Al_2O_3	420	0.175	162	40	~1000	0	OK
-C	Al_2O_3	420	0.3	150	20	~300	1	OK
-D	Al_2O_3	420	0	128	50	9	0	OK
-F	Al_2O_3	420	0.008	124	40	~400	0	OK
-G	Al_2O_3	420	0.150	143	21	42	3	OK
-M	Al_2O_3	420	—	--	--	—	--	No contact

Cathode	Mount	Bake Temp (°C)	Current Gate (mA)	Applied Voltage (V)	Emission (mA)	Tips Blown	Shorts	Notes
Group 17								
20A-110-1-B	TO-5	410	0	160	20	9	0	OK
-C	TO-5	410	0	160	20	75	0	OK
-V	TO-5	410	—	—	—	—	—	No contact
-D	TO-5	410	0.04	178	50	0	0	OK
-F	TO-5	410	0	160	20	2	0	OK
-G	TO-5	410	0	160	20	0	0	OK
Group 18								
20A-110-1-H	TO-5	410	0.012	195	20	~500	3	OK
20A-81-3-B	TO-5	410	0.006	165	22	~300	3	OK; cracked
-H	TO-5	410	0	160	22	~200	1	OK; cracked
-F	TO-5	410	0.008	180	48	~700	3	NG; cracked
-J	TO-5	410	4.5	135	95	~500	6	NG; seasoned
-G	TO-5	410	—	—	—	—	—	No contact
Group 19								
20A-107-5-B	Al_2O_3	440	0.43	225	10	~1000	2	NG
-C	Al_2O_3	440	0.075	230	22	~500	0	OK; poor
-D	Al_2O_3	440	0.005	220	20	~300	0	OK; poor
-F	Al_2O_3	440	0.125	235	20	~1000	0	OK; poor
-K	Al_2O_3	440	0.028	212	20	~300	0	OK; poor
-L	Al_2O_3	440	0.022	228	30	24	0	OK
Group 20								
20A-107-10-F	TO-5	410	0.002	166	10	3	0	OK
-G	TO-5	410	0	135	10	0	0	OK
-H	TO-5	410	0.002	142	10	3	0	OK
20A-112-5-G	TO-5	410	0.1	130	20	~300	2	OK; 2nd test damaged by ARC
-I	TO-5	410	0.1	155	20	~300	0	OK
(No cathode)								

Cathode	Mount	Bake Temp (°C)	Current Gate (mA)	Applied Voltage (V)	Emission (mA)	Tips Blown	Shorts	Notes
Group 21								
20A-111-1-B	TO-5	390	--	--	--	--	--	No contact
-C	TO-5	390	0.01	207	20	1	0	OK
-F	TO-5	390	0.008	200	20	0	0	OK
-D	TO-5	390	--	--	--	--	--	No contact
-G	TO-5	390	--	--	--	--	--	No contact
-H	TO-5	390	0.013	220	20	~500		OK; damaged by ARC
Group 22								
20A-111-3-A	Al_2O_3	300	0.003	162	20	30	1	OK
-B	Al_2O_3	300	--	--	--	--	--	No contact
-J	Al_2O_3	300	0.003	150	15	24	0	OK
-K	Al_2O_3	300	0.150	200	20	~500	0	OK; poor
-L	Al_2O_3	300	0.01	175	200	~200	2	OK; poor
-N	Al_2O_3	300	0.055	170	20	~200	1	OK; poor
Group 23								
20A-107-10-L	Al_2O_3	400	0.015	202	20	50	0	OK
-P	Al_2O_3	400	0.009	201	20	13	0	OK
-Q	Al_2O_3	400	0.009	195	20	2	0	OK
20A-110-1-J	Al_2O_3	400	0.032	200	50	5	0	OK
-K	Al_2O_3	400	0.02	215	15	2	0	OK
-N	Al_2O_3	400	0.01	62	20	1	1	Seasoned; NG
Group 24								
28A-118-3-B	TO-5	390	0.022	195	20	>100	1	OK
-C	TO-5	390	--	--	--	--	--	No contact
-D	TO-5	390	0.02	159	20	~100	1	OK
-G	TO-5	390	0.005	181	20	75	0	OK
-H	TO-5	390	0.005	160	20	32	0	OK
-I	TO-5	390	0.006	200	20	~100	1	OK